



Water Inrush Modes Through a Thick Aquifuge Floor in a Deep Coal Mine and Appropriate Control Technology: A Case Study from Hebei, China

Chunyuan Li¹ · Jianping Zuo² · Xuanhao Huang³ · Genshui Wu² · Yubao Li⁴ · Shikun Xing⁵

Received: 13 July 2021 / Accepted: 13 July 2022 / Published online: 2 August 2022
© The Author(s) under exclusive licence to International Mine Water Association 2022

Abstract

Water inrush disasters caused by confined aquifers under high pressure below the mine floor are a major problem in China, restricting the safe and efficient mining of deep coal seams. We have classified the stress disturbance modes acting on the floor area in such mines into two types based on the water yield changes of a thick aquifuge floor in a deep longwall mine and the underground pressure behavior of deep longwall faces during water inrush events, and they are the dynamic load of the main roof instability from the far field of the longwall face and the static load of the abutment pressure from the near field, respectively. The water inrush modes include mining-induced cracks indirectly connected with the Ordovician limestone aquifer and through-going faults directly connected with the same aquifer. In order to control water inrush from thick aquifuge floor, grout was used to block off the cracks in the strata just above the Ordovician limestone on the site; decreasing the mining width also decreased the stress disturbance intensity caused by the dynamic and static loads; while presplitting the roof relieved the underground pressure and effectively weakened the dynamic load; and the confined water was drained to lower the water pressure and cut off the source of water flowing into the longwall face. Finally, the combined effectiveness of these control technologies was verified by micro-seismic monitoring, and further water inrush disasters were prevented through the thick aquifuge floor of a deep longwall mine in the Xing-dong coal mine in north China.

Keywords Water inrush · Stress disturbance · Control technology · Thick aquifuge floor · Deep longwall mining

Introduction

In China, most coalfields have moved towards deeper coal mining. However, the hydrogeological conditions of deep coal are extremely complex, with greater in-situ stress and karst fissure water pressure. Water inrush events still occur, even when the aquifuge is very thick, restricting safe and efficient mining.

Currently, floor failures are identified by field observations of the water inrush mechanism and hydraulic conductivity enhancement is analyzed by the finite element method coupled with stress-dependent permeability (Zhang 2005). With consideration of the effects of mining pressure and the non-uniformly distributed hydraulic pressure, Liang et al. (2020) used a hydraulic–mechanical calculation model to analyze the theoretical range of failure and the stability of inclined floor strata after mining. Lu et al. (2018) obtained the reliability probability of the floor by establishing two modes of water-resistant floor failure. Li et al. (2016) studied the “triangle” water-inrush mode of a strong water-guide collapse column

✉ Chunyuan Li
lcy6055@163.com

✉ Jianping Zuo
zjp@cumtb.edu.cn

¹ Deep Mining and Rock Burst Research Institute, China Academy of Coal Science, Beijing 100013, China

² School of Mechanics and Civil Engineering, China University of Mining and Technology (Beijing), Beijing 100083, China

³ School of Energy and Mining Engineering, China University of Mining and Technology (Beijing), Beijing 100083, China

⁴ Hebei Coal Research Institute, Hebei, Xingtai 054000, China

⁵ Xingdong Mine, Jizhong Energy Group Corporation Ltd., Hebei, Xingtai 054000, China

by using similar simulation tests and numerical simulation software. Many studies on the water inrush mechanism have concentrated on the failure depth (Huang et al. 2016; Zhai et al. 2019), mining faults (Mu et al. 2020; Sun et al. 2019), and evaluation methodology (Xiao et al. 2020; Yin et al. 2019) of floor areas in longwall mines. Some scholars have attempted to study the water inrush mechanism using methods such as three-dimensional numerical calculations (Li et al. 2020; Li and Bai 2020; Yu et al. 2020), comprehensive geophysical exploration (Xu et al. 2020; Yin et al. 2015), or similar simulation tests (Chen et al. 2020; Zhao et al. 2020). These studies provide a theoretical basis for studying the expansion and evolution of floor cracks and water-inrush channels in deep coal mines. However, they mostly focus on the water inrush mechanism of thin aquicludes in the floor area of shallow longwall mines, rather than a thick aquiclude floor under high-stress conditions in deep mines. Thus, the water inrush modes of a thick aquiclude floor induced by deep longwall mining requires further study.

Many scholars have also studied technologies for controlling water inrushes. Hu and Zhao (2021) reviewed the evolving trend of water disaster control technology. Liu et al. (2019) constructed a Bayesian network structure chart of water inrush risk and proposed a fuzzy probability risk analysis model to derive a reasonable risk control scheme for a water inrush. Wu et al. (2011) analyzed the typical cases of an inrush from the coal seam floor in the Huaibei mining area and how to control the rock mass structure. Li et al. (2012) designed a water prevention and control plan for limestone water below the mine. Zou et al. (2010) identified a water-rich area by seismic impedance inversion and underground transient electromagnetics and then carried out a grouting reconstruction project on the local coal floor. These studies enrich the water inrush control technologies and support safer mining in deep coal mines. However, there are some deficiencies in complicated geological condition, high confined water pressure, and dynamic risk changes, and so new prevention and control methods are needed to prevent water inrushes through the floor area in deep longwall mines.

This paper analyzes the water inrush modes of thick aquifuge floors in deep longwall mines considering the typical geological engineering and underground pressure characteristics of north China's coalfields. The stress disturbance modes acting when mining above high-pressure confined water were studied. Overall, this paper provides technical support for safe and efficient mining in deep coal mines.

Water Inrush Modes of Thick Aquifuge Floor in Deep Coal Mines

The Xing-dong coal mine, located in Xingtai city in the Hebei Province of China has a vertical shaft and multi-level development. The mining level ranges from –760

to –980 m. To date, water inrush in the floor area has not occurred at the shallow –760 m level. However, water inrush has occurred at five of the ten longwall faces mined at a depth of –980 m; of the five that have not suffered water inrush through the floor, one face had adopted water inrush control technologies. The water inrush modes through the mine floor exhibit certain differences in response to the nature of the underground pressure.

Geological Engineering Characteristics of the Xing-dong Mine

The #2 coal seam is being mined at the –980 m level using a fully mechanized large-height longwall method along the strike. The coal is cut by an MG500/1140-WD electric haulage machine, the roof is supported by ZY5000/25/50-type hydraulic supports with two shield columns, and the goaf is dealt with by the caving method. The depth of the #2 coal seam is 1000–1275 m, and the thickness of the coal seam is 3.2–4.6 m. The dip angle of the coal seam is about 10–15°, although this can change significantly due folds and faults. The geologic column at –980 m is shown in Fig. 1.

The Yeqing, Fuqing, and Daqing limestone aquifers are, respectively about 46.3, 96.0, and 149.4 m below the coal seam. These three limestone aquifers are the main components of the mine's normal water inflow; their inflow totals about 25 m³/h, occasionally rising to 30 m³/h. Their water yield is low, easily drained, and is generally not considered dangerous. However, there is a very thick Ordovician limestone aquifer about 170 m below the #2 coal seam that has a strong and non-uniform water yield, which means it cannot be drained. The water supply is steady, the water reserves are large, and the confined water pressure ranges up to 14.7 MPa. Moreover, the #2 coal seam is divided by severe normal faults that are widely distributed in this mine field.

The mining sequence of longwall faces at the –980 m level is 2121, 2123, 2122, 2127, 2124, 2222, 2125, 2126, 2228, and 2129. The layout of the longwall faces is shown in Fig. 2 and the mining parameters of several longwall faces are presented in Table 1. Among these longwall faces, the most serious in terms of water yield is longwall face 2228, where the peak water yield reached 2649 m³/h. The SF₂₇ fault group was discovered where the mining line and track roadway met in longwall face 2228. The depth of the coal seam is about 1000 m and the water pressure of the Ordovician aquifer is up to 10.2 MPa. Before mining, all longwall faces were synthetically surveyed using the direct current electric method, channel waves, transient electromagnetism, drilling exploration, and other methods.

Fig. 1 Synthetic geological section at –980 m level

Column	Rock stratum and lithology description	Layer thickness / m	Unit water inflow / (10 ³ L/S·m)	Permeability coefficient / (10 ⁻² m/day)
		Minimum-maximum Average	Minimum-maximum Average	Minimum-maximum Average
	Sandstone, siltstone, and medium-fine sandstone are composed.	$\frac{6.90-39.90}{19.83}$	$\frac{1.44}{1.44}$	$\frac{0.353}{0.353}$
	The main rock is siltstone, in which contain 1-3 layers of thin coal seam.	$\frac{19.09-48.12}{34.56}$		
	The rock is sandstone, in which fractures are developed, and its thickness varies greatly.	$\frac{0.99-16.03}{8.05}$	$\frac{1.04-1.08}{1.06}$	$\frac{0.72-1.19}{0.955}$
	Siltstone and medium sandstone contains 3-4 layers of coal.	$\frac{42.54-67.90}{53.16}$		
	The rock is Yeqing limestone, in which fractures do not develop.	$\frac{1.27-4.26}{2.23}$	$\frac{3.56-3.82}{3.69}$	$\frac{14.2-17.8}{16.0}$
	The main rock is siltstone, in which contain several layers of coal.	$\frac{28.56-49.73}{41.01}$		
	The rock is Fuqing limestone, in which fractures do not develop.	$\frac{0.63-3.26}{1.95}$	$\frac{2.63-2.97}{2.80}$	$\frac{11.1-20.1}{15.6}$
	The main rock is siltstone, in which fractures are developed.	$\frac{24.56-59.57}{36.36}$		
	The rock is Daqinglimestone, with 1-2 layers of fine sandstone.	$\frac{1.70-8.22}{5.34}$	$\frac{1.41-4.32}{0.921}$	$\frac{9.25-41.4}{25.3}$
	The upper is the thick coal seam, the middle is the aluminum siltstone.	$\frac{4.69-33.76}{20.91}$		
	The rock is Benxi limestone, in which fractures do not develop.	$\frac{0.00-8.88}{3.49}$		
	The rock is Aluminosilite siltstone, which contains fine sandstone.	$\frac{2.93-38.0}{5-10}$		
	The rock is thickly layered Ordovician limestone with wavy or horizontal bedding, in which cracks and small karst caves are developed. Water leakage and water inrush are common through boreholes in this layer.	$\frac{45.23-94.59}{65.03}$	$\frac{38.2-3776}{1046}$	$\frac{7.16-745}{184}$

No shallower faults or dense fracture zones were discovered within 60 m of the coal seam.

Water Inrush Modes Through a Thick Aquifuge Floor in Deep Coal Mines

At the 2125 longwall face, the position of the water inrush was located near the junction of the stopping line and the tail entry. Mining stopped, and the longwall face was sealed after the inrush through the floor occurred. The water yield was 4.98–79.8 m³/h during mining. Later water inflow data were not recorded in detail. Therefore, the water inrush modes in the floor area are only analyzed for longwall faces 2126, 2127, 2222, and 2228 at the deep –980 m level. The changes in water level in the hydrological boreholes near these faces and the water yield are shown in Fig. 3.

The 2126 Longwall Face

Before the inrush occurred in the 2126 longwall face, the water level in the no. 4 borehole, some 1000 m away from the open-off cut, declined abnormally over the previous 15 days. It declined 0.014 m 11 days before the inrush and had declined a cumulative 0.485 m four days before the inrush occurred. Then, the water level declined 4.751 m over the following 35 days.

As the 2126 longwall face advanced about 316 m, water inrush occurred through the floor area near the mining line and tail entry. Afterwards, the 2126 longwall face advanced 197 m in total, at an average velocity of about 1.8 m per day. The initial water yield was 30 m³/h. As the water inrush continued, the water yield increased to 70 m³/h within 3.5 h. Later, it maintained a level of 80–130 m³/h. After about

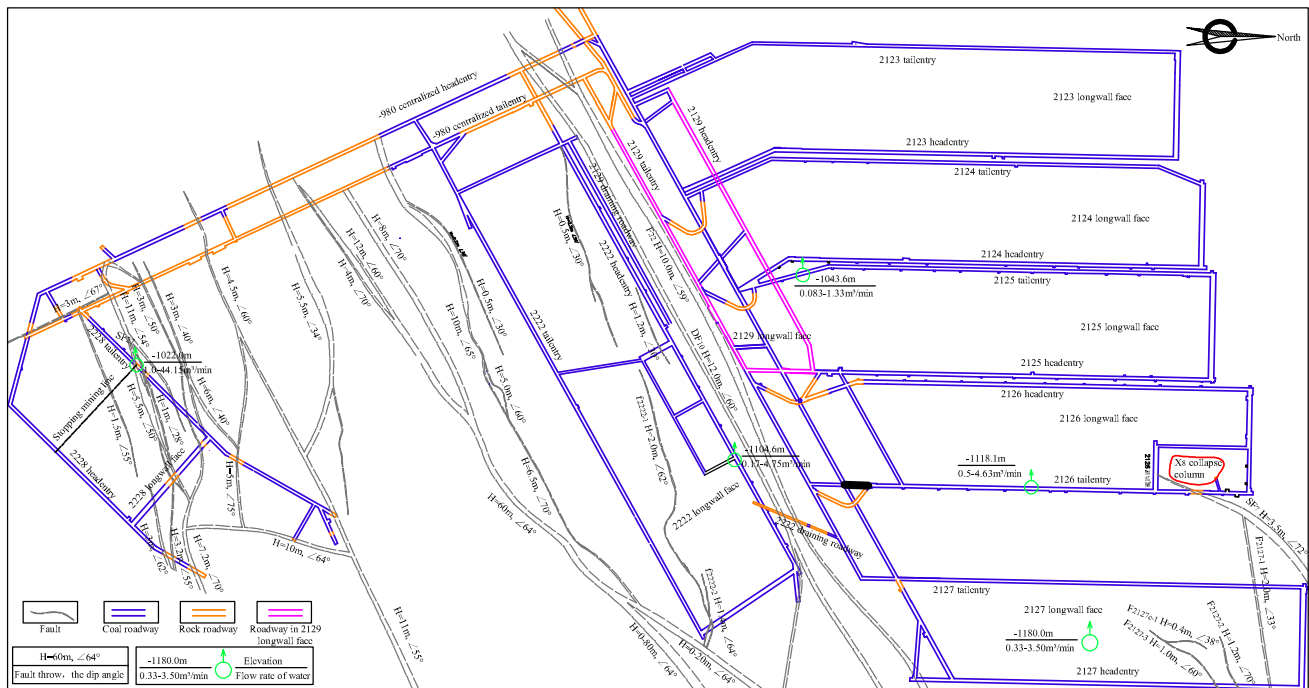


Fig. 2 Longwall face layout at –980 m level

Table 1 Technical mining parameters and water inrush characteristics at –980 m level in Xing-dong mine

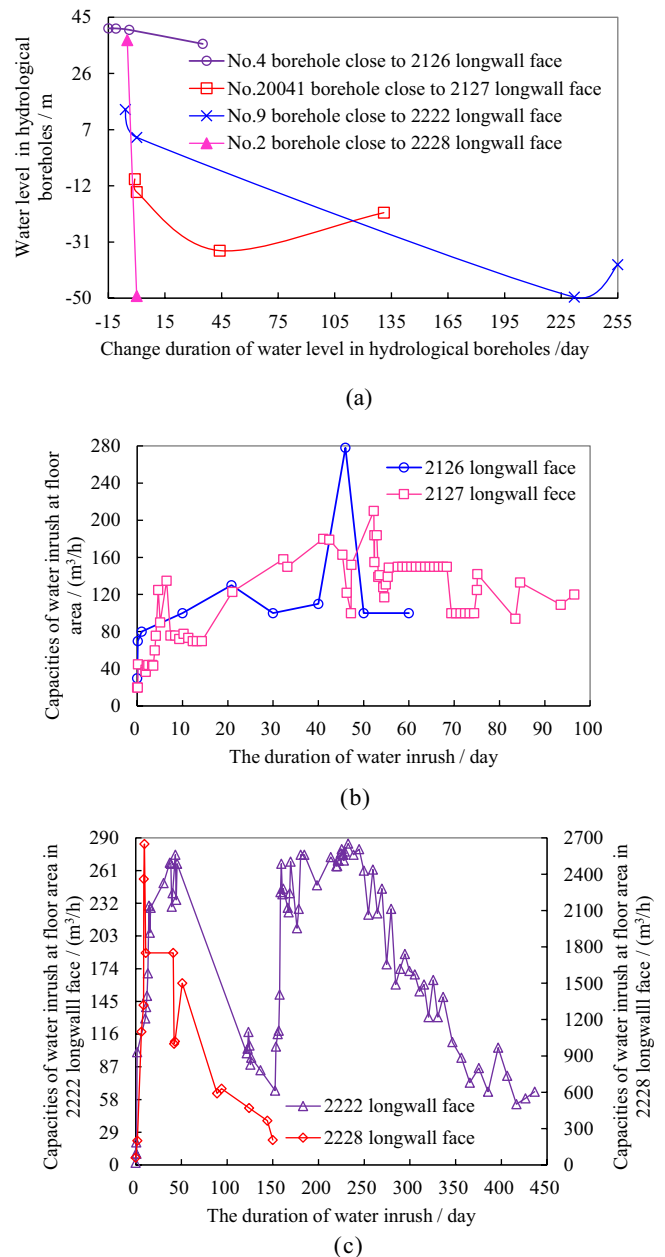
Name of longwall face	Strike length/m	Mining width/m	Inclination/°	Burial depth/m	Mining height/m	Water pressure/MPa	Thickness of aquiclude /m	Maximum of water yield/(m ³ /h)
2125	548	148	6–23	1091–1185	3.7–4.6		174	79.8
2126	530	145	3–13	1116–1215	3.6–4.5	12.7–13.8	174	278
2127	541	141	12–15	1184–1275	3.1–4.7	14.0–14.7	175	210
2129	391.5	92.8	9–14	1127–1225	3.8–4.1	12.0–13.0	180	No water inrush
2222	711	162	10–18	1136–1239	3.2–4.2	10.0–13.3	180	285
2228	249.5	165	16–22	1132–1235	3.5–4.2	10.2–13.1	172	2649

46 days of water inrush, the peak value of the water yield was 278 m³/h. The water yield then decreased gradually and maintained a level of around 100 m³/h. According to the characteristics of the water yield in the floor area, the floor-area fracture in the 2126 longwall face did not directly connect with the Ordovician aquifer. Only when mining-induced cracks developed in the floor area did the water inrush reach its peak value, and this lasted a long time as the water yield stabilized from a small to a large value, suggesting that the water inrush had buffering and durative characteristics. Therefore, the water-conducting channel from the Ordovician aquifer must have been partially blocked. It may be speculated that crack structures in the deep floor connected with mining-induced cracks in the shallow floor, causing the water inrush to occur.

The 2127 Longwall Face

In the 2127 longwall face, four faults were discovered before the water inrush occurred. These faults are named F₂₁₂₇₋₁, F₂₁₂₇₋₂, F₂₁₂₇₋₃, and F_{2127c-1} and have drop heights of 1.7, 1.2, 1.0, and 0.4 m, respectively. The 2127 longwall face had advanced 300 m outside the open-off cut when the water inrush happened, and the position of the inrush was 80 m away from the pinch-out section of the outermost discovered fault. One day before the inrush occurred, the water level in borehole no. 20041, located a horizontal distance of 800 m from the point of water inrush, obviously decreased. The water level fell to –14.084 m prior to the inrush and declined by 4.38 m in one day. After the water inrush had continued for 44 days, the water level had decreased to a

Fig. 3 Changes in water yield and level in hydrological boreholes near the ground in deep coal mining: **a** Changes in the water level of hydrological boreholes; **b** Longwall faces in 21st district; **c** Longwall faces in 22nd district



minimum of -33.917 m, and the drawdown water level reached 19.833 m. Due to the water inrush, the 2127 longwall face had to stop mining four times, and the total yield of the inrush was about $400,000$ m³.

Initially, the water inrush began to flow out from the goaf behind the head entry. The water yield was about 20 m³/h with gas overflow, and the water was muddy and smelly. The concentration of hydrogen sulfide in the surface water reached 70 ppm. After about 5 h, the water yield clearly increased, and the water flowed out from push rods of hydraulic supports 8 , 15 , and 42 . The total water yield was 40 – 50 m³/h at the position of the reversed loader in the head entry. Mining then stopped at this longwall face and the

water was cleared. However, as the longwall face advanced, the water yield presented an obvious saltatory increase. For instance, the water yield increased rapidly from 44.3 to 125 m³/h three days after the water inrush began and increased rapidly from 100 to 210 m³/h after about 47 days. The maximum water yield was 210 m³/h in the 2127 longwall face, which is not particularly high. This indicates that the fracture cracks in the floor area did not directly connect with the Ordovician aquifer; instead, the water flow channel was indirect or impeded. It is also possible that the Ordovician aquifer indirectly connected with the mining-induced cracks because of the existence of crack structures in the deep floor, and this caused the water inrush.

The 2222 Longwall Face

Six days before the water inrush began, the water level in borehole no. 9 declined abnormally. This borehole is located 724 m away from the open-off cut of the 2222 longwall face. The rate of decrease was about 423 mm/h, much faster than historical values and greater than in an observation borehole near borehole no. 9. When the water inrush occurred, the water level in borehole no. 9 declined by 9.4 m. After about seven months, at the end of mining, the water level reached its lowest level, a cumulative decrease of around 62.806 m. Moreover, two faults (f_{2222-1}^- and f_{2222-2}^-) with drop heights of 1.4 and 2 m, respectively, were discovered prior to the water inrush. The two faults extended to the middle of the longwall face from the tail entry. Water inrush occurred when the longwall face had advanced 178.8 m. Mining of this face stopped two times and advanced 490 m in total, and the total water yield was about 1,480,000 m³.

When the water inrush happened, the water flowed out in front of the bed plate of hydraulic support 82. The water yield was about 2 m³/h. After 4.8 h, there was one new point of water inrush at hydraulic support 66, and the total water yield was about 10 m³/h. After 16 h, the water flowed out at hydraulic supports 50, 66, 83, 87, and 93 with various water yields, and the total water yield gradually increased to 20 m³/h. After 20.3 h, the water flowed out from the floor at the upper end of the head entry; the initial water yield was about 10 m³/h, and this gradually increased. Mining stopped and measures such as excavating the drainage roadway, excavating the open-off cut, and throwing away hydraulic supports were taken. The mining then continued. The maximum water yield of 275 m³/h occurred 43 days after the water inrush began; the water yield gradually decreased to 66 m³/h after 152 days. Later, the water yield increased again, and maintained a level of 200–285 m³/h. The maximum of 285 m³/h occurred after 232 days, before decreasing again. Therefore, the water inrush in the 2222 longwall face had two clear stages. The difference in the maximum water yield of each stage was only 10 m³/h. However, the duration of the maximum water yield was relatively short in the first stage (≈ 30 days), and almost 2.5 times longer in the second stage (≈ 84 days). The measures taken after the water inrush began and the stopping of mining operations reduced the disturbance of mining-induced stress, lowered the likelihood of cracks and fractures in the floor area, and decreased the chance of mining-induced cracks connecting with the Ordovician limestone aquifer in the deep floor area. These factors acted to gradually reduce the water yield. In the second stage, the inclined length of the longwall face was recovered to that of primary mining, and the crack network and fracture depth in the floor increased due to the mining disturbance. This strengthened the ability of mining-induced cracks to connect with the Ordovician limestone aquifer in

the deep floor area. The maximum water yield gradually decreased after mining operations had passed through this section. Moreover, fault F_{22} was discovered during mining in the middle of the longwall face, with four minor faults nearby. Together, these faults constituted the weakest zone. The main position of water inrush changed outside the lower end of the tail entry. There was little water in other positions after water began to flow at the lower end of the tail entry. Under the upfaulted drop and lifting of the footwall of faults DF_{10} and F_{22} , the vertical distance between the fracture zone in the floor area in the 2222 longwall face and the Ordovician aquifer decreased, and the confined water of the Ordovician aquifer reached a pressure of 13.3 MPa. This caused the water in the Ordovician limestone to invade the fracture zone along the weak surface of the faults. At the lower end of the tail entry, the water was very muddy, indicating a fault gouge. This shows that fault F_{22} and its derivative minor faults did not directly connect with the Ordovician aquifer in the floor area; cracks in the floor area connected with fault F_{22} and its derivative minor faults, which activated F_{22} and its derivative minor faults. As crack structures in the deep floor connected, cracks in the shallow floor indirectly connected with the Ordovician aquifer.

The 2228 Longwall Face

Five days before the water inrush occurred in the 2228 longwall face, the water level in borehole no. 2, 1600 m away from the position of water inrush, declined abnormally from 37.244 m. Around 26.5 h before the water inrush began, the water level began to decline rapidly; by the time the water inrush occurred, the water level had declined to -49.233 m, a cumulative decrease of 86.477 m. The water source was confined water in the Ordovician limestone.

About 12.5 h before the inrush began, periodic weighting occurred where the tail entry had advanced about 148.7 m. When the water inrush happened, the SF_{27} fault group was at the intersection of the mining line and tail entry; intense periodic weighting occurred again, and the pressure on the hydraulic supports increased rapidly. The floor heaved near the end of the tail entry, the water yield rose to about 60 m³/h, and mining was stopped on the 2228 longwall face. As the inrush continued for a day, the water yield gradually increased to 200 m³/h; after about five days, it was 1100 m³/h; after nine days, it quickly increased to 2360 m³/h from 1319 m³/h within the space of 4 h; after 10 days, it reached a maximum of 2649 m³/h. The water yield then gradually decreased and stabilized at about 1750 m³/h after two days. About 42 days after the inrush began, the water yield had decreased to less than 1000 m³/h; over the period from 42–57 days after the water inrush began, the water yield had basically stabilized at about 1000 m³/h, although it increased to 1020 and 1500 m³/h on separate occasions due to grouting

activity. As the grouting continued, the water yield fluctuated and then stabilized at 205 m³/h. Therefore, the water yield in the floor area in 2228 longwall face was far greater than that when mining-induced cracks connected with crack structures in the deeper floor. Due to the intersection of the mining-induced shear fracture zone and the through-going fault in the 2228 longwall face, the faults connected with the Ordovician aquifer, and the large-scale abrupt water inrush occurred.

Therefore, the maximum water yield was only 210–285 m³/h in the 2126, 2127, and 2222 longwall faces, where it took at least 43 days to reach the maximum; the water conduction channels were blocked, and the inrush had buffering and durative characteristics. The mining-induced cracks indirectly connected with the Ordovician limestone aquifer in the deep floor area. However, the yield of the 2228 longwall face inrush reached a maximum of 2649 m³/h within 10 days, and it occurred at the intersection region between through-going faults and the coal rib of the longwall face. Hence, the 2228 longwall face water inrush was due to through-going faults directly connected with the Ordovician limestone aquifer. Due to the vertical distance of 170 m between the Ordovician limestone and the #2 coal seam, the incubation time of cracks fracture and connection in the thick aquifuge floor increased, and the maximum water yield lagged by more than 10 days.

Stress Disturbance Modes Acted on the Floor Area in Deep Coal Mining

The underground pressure behavior of each longwall face at the –980 m level was observed during water inrush, and these data can be used to study the dominant stress disturbance modes of the fractures. Before the water inrush occurred, the 2127 longwall face had advanced 300 m and there was no obvious underground pressure during mining. During the inrush, the underground pressure increased dramatically. The load data from the 98 hydraulic supports were steadily sampled at 4 h intervals in the 2127 longwall face over a period of 81 days. The support loads and advance speed changes in 2127 longwall face are shown in Fig. 4.

Compared with Fig. 3b, there are obvious correlations between water inrush in the floor area and periodic weighting in the 2127 longwall face. When the support loads were high, the advance speed obviously decreased. After the inrush had gone on for three days, 21 hydraulic supports were crushed, 26 columns and 16 balance jacks were squashed, and the beam pits of columns on six supports and the bed plate pits of columns on four supports were perforated. During the 67 days after the inrush began, the periodic weighting interval was 10–15 m; after more than 67 days, it was about 20 m. As the longwall face advanced, the water yield abruptly increased. This meant that the water yield

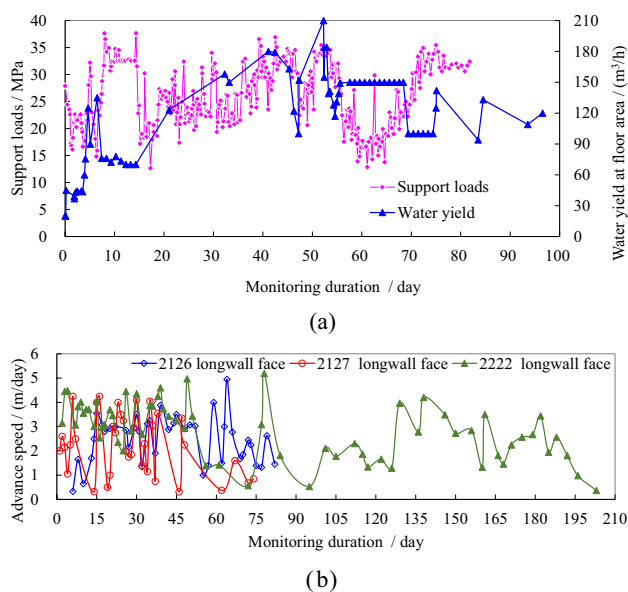


Fig. 4 Support loads and advance speeds at different longwall faces: **a** Support loads and water yields at the 2127 longwall face; **b** Advance speed changes at different longwall faces

notably increased with the underground pressure, and the water inrush in the thick aquifuge floor was induced by the dynamic loads of the main roof instability from the far field of the longwall face. As the periodic weighting occurred, cracks within the fracture depth of the shallow floor opened. Thus, the water flow channels in the floor area were relatively unimpeded and water in the cracks behind the longwall face first flowed into the cracks in the shallow floor. Once the cracks in the shallow floor filled with water, the water flowed out from the coal rib, which indicates that the water flowed out in front of the hydraulic supports slowly after the water level in borehole no. 20041 had descended for some time. As the underground pressure increased, some cracks in the shallow floor closed, partially obstructing the water flow channels. At this point, the water yield gradually decreased, most water flowed out from the goaf, and the water level in borehole no. 20041 increased slightly, as shown in Fig. 3a. Therefore, the dynamic loads of the main roof instability played an important role in the fracturing of rock masses in the floor area, which caused fracture cracks in the shallow floor to connect with crack structures in the deep floor. Thus, the water inrush was indirectly induced by fracture cracks connected to the Ordovician aquifer.

Similarly, periodic weighting occurred frequently in the 2228 longwall face during the initial water inrush, and the increase in underground pressure was obvious. Due to the complex structures of the mining area, more than 13 faults were discovered in the 2228 longwall face, with cracks developing and strata fracturing near the faults. When the longwall face was unaffected by mining, the water pressure

in the Ordovician limestone reached 10.2 MPa but did not break through the aquiclude; the water also did not flow out in advance from the detection boreholes in the floor area. However, based on detection data from the no. 2 grouting borehole in the tail entry and head entry, the drop height of the SF₂₇ fault group in the Ordovician aquifer was more than that in #2 coal seam, and this caused the distance between the Ordovician aquifer and #2 coal seam to decrease. Under the dynamic load disturbance of the main roof instability, the fracture depth increased and the SF₂₇ fault group became fractured. The SF₂₇ fault group then directly connected with the Ordovician aquifer. Thus, the water inrush was induced by the through-going fault under dynamic loads.

During the inrush in the floor area of the 2126 and 2222 longwall faces, the water yield was relatively low, and there was no obvious periodic weighting. The water yield did not obviously increase with respect to the underground pressure. Moreover, it took a long time for the water yield to increase and stabilize, and the inrush exhibited buffering and durative characteristics. Hence, the water-conducting channel of the inrush from the Ordovician aquifer was partially blocked. Under the static loads of the abutment pressure from the near field of the longwall face, the inrush was mainly induced by the indirect connection of cracks in the shallow floor and the growth and conductive crack structures in the deep floor.

Thus, the stress disturbance modes on the floor area in deep coal mining can be divided into two types. One is the dynamic load mode of the main roof instability from the far field of the 2127 and 2228 longwall faces. Another is the static load mode of abutment pressure from the near field of the 2126 and 2222 longwall faces. Under these two modes, the inrush through the thick aquifuge floor was induced when the fracture cracks connected with the Ordovician aquifer.

Water Inrush Control Technologies in Deep Coal Mines

Grouting and Reinforcement with Horizontal Branch Boreholes in the Floor Area

Directional horizontal boreholes were used to grout and reinforce the top strata of the Ordovician aquifer at the –980 m level. This mainly involved operating long-distance horizontal branch boreholes on the ground. The karst cracks of the aquifer on top of the Ordovician limestone were transformed into a relative aquiclude, blocking off the connection between the Ordovician aquifer and the mining-induced cracks. The aim was to control the water inrush through the deep longwall mine floor above the high-pressure confined water.

The horizontal branch boreholes on the ground are composed of one inclined straight main borehole, two directional horizontal boreholes, and horizontal directional branch boreholes. The bottom of the main borehole extended 25 m into the Ordovician limestone. The horizontal directional branch boreholes were drilled along the bedding of the strata and were divided into the N1 borehole group in the north area and the S1 borehole group in the south area. The drilling project was divided into five stages based on the replacement of the longwall faces. The drilling order of each stage is described in Table 2.

The bottom of the directional horizontal boreholes from the first stage to the fourth stage were drilled 70–100 m into the Ordovician limestone; the horizontal distance between boreholes was 70 m. According to the leakage during drilling, the karst cracks of the Ordovician limestone aquifer had developed a layered feature from 70–90 m below the top surface of the Ordovician limestone; this was not the case for the strata 90–130 m from the top surface of the Ordovician limestone. The karst cracks in the Ordovician limestone exhibit widespread development at the –980 m level.

Table 2 Drilling order of the nearly horizontal boreholes

Stage	Location	Drilling order	Purpose of drilling
First	North Area	N2, N1, N3, N7	Cover the floor at north area at 2125 longwall face; operate horizontal borehole alternately
Second	North Area	N8, N9, N10, N11, N12, N13	Cover the floor at 2224 longwall face; govern the water inrush positions at 2222 longwall face
Third	North Area	N4, N4t, N4t-1, N5, N6, N6t, T1	Covering 2126 longwall face and the area between 2127 longwall face and the gangue filling roadway at –980 m level
Fourth	South Area	S1, S2, S3, S4, S5, S6, S7, S8	Cover the floor in 2226 and 2228 longwall faces
Fifth	2129 longwall face	T1–T14, 14 boreholes in total	Extend 220 m toward the south side of 2129 longwall face, extend 90 m toward the north side of 2129 longwall face, near the open-off cut, extend 93 m outside of the stopping line, encircle all floor areas in 2129 longwall face, and utilize all previous boreholes

They are small, poorly connected, and the high pressure of the water causes more fractures and connections between cracks; some cracks are well-developed and can easily connect within local areas.

After the first four stages of grouting reinforcement, water inrush disasters continued to happen during mining of the 2125, 2126, and 2228 longwall faces, and so the reinforcement effect in these areas was not obvious. To guarantee the safety of mining in 2129 longwall face, the horizontal distance between boreholes was adjusted to 60 m in the fifth stage, and the strata of grouting reinforcement was changed to less than 50 m below the top surface of the Ordovician limestone. The areas of grouting reinforcement encircled the floor area of the 2129 longwall face and used all previous boreholes, as shown in Fig. 5.

According to Fig. 5, 14 boreholes were constructed in the 2129 longwall face, numbered T1–T14. The intended strata for T1–T4, T7, and T8 were about 70–90 m below the top surface of the Ordovician limestone aquifer, and the intended strata for T5, T6, and T9–T14 were 10–50 m below

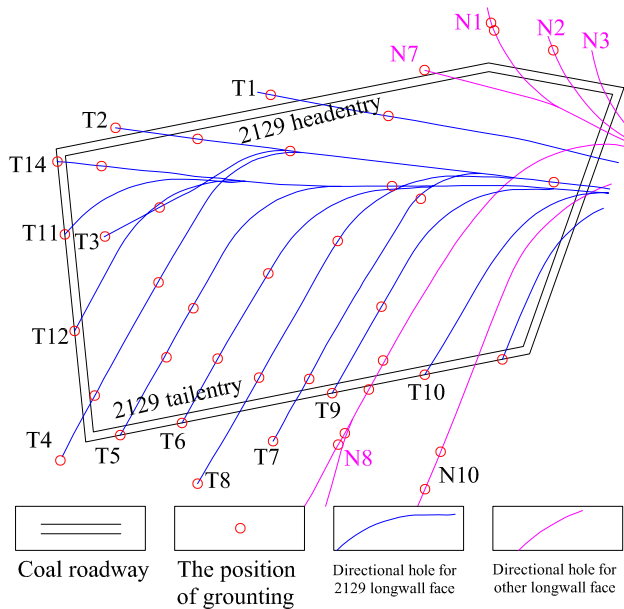
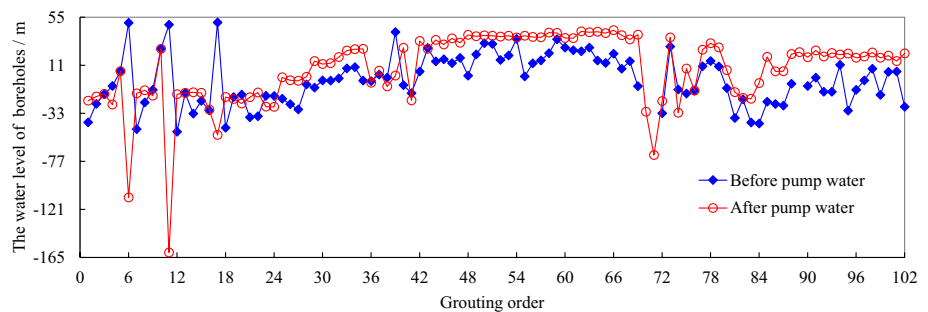


Fig. 5 Distribution of grouting positions at the 2129 longwall face

Fig. 6 Water level in boreholes before and after pumping



the top surface of the Ordovician limestone aquifer. Six pre-constructed boreholes (N1, N2, N3, N7, N8, and N10) covered the corner areas of 2129 longwall face; their intended strata were 78–117 m below the top surface of the Ordovician limestone aquifer. Therefore, weak planes of cracks, and the aquifer in the deep floor of the 2129 longwall face were grouted and reinforced at different spatial levels.

Grouting was carried out 98 times from the first borehole (N2) to the last borehole (T10). All boreholes were pumped with water to wash the well and the water level was observed each time. There are 201 groups of data in total for the water level of the Ordovician aquifer. The water levels in the boreholes before and after pumping are shown in Fig. 6.

The water level in the boreholes generally rose after the well was pumped and washed, although several individual boreholes saw significant decreases. Hence, the Ordovician water flow channels were unblocked after pumping and the water level was much closer to the real situation. During the 25th grouting in borehole N9, on August 5, 2016, the water level rose above the previous level; this was caused by heavy rainfall from July 19, 2016. At the beginning of the final grouting in borehole T4, on March 12, 2018, the water level declined and fluctuated, mainly because of the inrush and the governing process in the 2228 longwall face. Therefore, the Ordovician water flow channels performed better in the local floor at the –980 m level, which further explains why cracks developed in the deep floor.

Decreasing Mining Width

Ignoring the influences of grouting reinforcement, roof presplitting, and dynamic drainage, the relationship between water inrush through the floor and the mining width of the longwall faces at the –980 m level is shown in Fig. 7. Figure 7 shows that all inrush events happened when the mining width was greater than 140 m; the maximum mining depth was 1225 m in the 2129 longwall face, but its mining width was only 92.8 m (66.29% of 140 m), and no water inrush occurred during mining. Although grouting reinforcement, roof presplitting, and dynamic drainage were adopted in 2129 longwall face, the relatively low mining width also likely played a part in this.

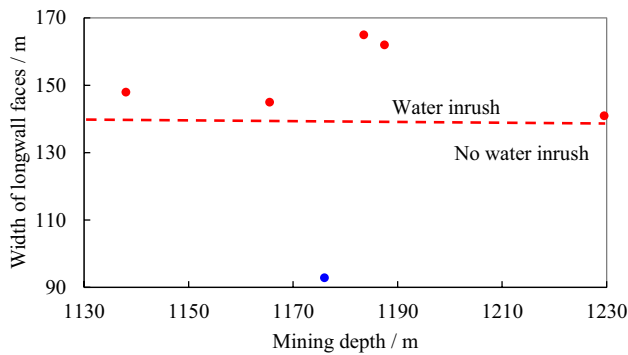


Fig. 7 Relationship between water inrush at floor area and mining width of longwall faces at –980 m level

Based on the fracture depth data of the floor area measured and collected onsite, Xu and Yang (2013) applied regression analysis according to:

$$h_1 = 0.042H - 0.416\alpha_L + 0.013L - 3.276M + 7.255 \quad (1)$$

where h_1 is the fracture depth in the floor area, α_L is the dip angle of the coal seam, and L is the mining width of the longwall face. In Eq. (1), the fracture depth of the floor area and the mining width are positively correlated, that is, a greater mining width suggests a deeper fracture depth, which is beneficial for water inrush through the floor. Hence, the wider the mining, the greater the stress disturbance intensity under static loads from the near field and dynamic loads from the far field. As the mining depth decreases, the abutment pressure in front of the longwall face and the lateral abutment pressure from the near field will decrease, which effectively decreases the fracture distance of the main roof. Thus, the disturbance intensity of the dynamic load caused by main roof breakage will decrease. Therefore, the mining width should be decreased as the mining depth increases to control water inrush through the floor.

Presplitting the Roof for Pressure Relief

To control the fracture distance of the main roof instability and lower the stress disturbance intensity of the floor caused by dynamic loads on the main roof from the far field, the main roof was presplit to release pressure in an attempt to control the inrush in the floor area in the 2129 longwall face. Boreholes were drilled in the roof on both sides of the roadway. The arrangement of the boreholes is shown in Fig. 8, where pink indicates the initial drilling plan and blue indicates the additional drilling plan according to the relief pressure.

There were 10 A-type boreholes and 10 B-type boreholes in both roadways. The elevation angle of the A-type

boreholes was 30°, and the drilling length was 50 m. The elevation angle of the B-type boreholes was 40°, the angle of intersection with the roadway was 10°, and the drilling length was 40 m. The diameter of the boreholes was 56 mm. The drilling velocity was decreased during drilling and the feeding force of the drilling machine was reduced, which ensured good linearity. As a result of using this technology, no drastic weighting occurred during mining of the 2129 longwall face; it effectively weakened the effect of dynamic loads caused by the main roof instability.

Dynamic Drainage of Confined Water in the Floor Area

Dynamic drainage of the confined water reduced the confined water pressure in the floor area, effectively cutting off the source of water. The inrush water was drained to the sump, thus avoiding an inrush through the floor.

The 2129 drainage roadway was dug near the 2222 head entry, as shown in Fig. 2. Due to the advantage of upward mining of the 2129 longwall face, the floor water drained to the sump during mining, which avoided the confined water flowing out from the coal rib. The hourly and total water discharge of the water pump in the 2129 draining roadway was recorded over 96 days before mining of the 2129 longwall face stopped (Fig. 9).

The changes in water discharge were similar to those in the supports loads as the 2129 longwall face advanced, although the period of the changes was smaller. During the monitoring time, the maximum hourly water discharge was 96.18 m³/h and the minimum was 34.00 m³/h; the longest drainage time was 30.83 h per day for all of the pumps, and the shortest drainage time was 4.3 h. The total water discharge was 146.2 m³ on the first day, rising to more than 607.49 m³ on all other days, and reaching a maximum of 2965.57 m³. Under the dynamic drainage and water pressure relief, the confined water in the floor area was effectively prevented from flowing out from the coal rib during mining of the 2129 longwall face. Thus, this action realized the purpose of controlling the water inrush through the floor.

Effectiveness of Water Inrush Control Technologies in Deep Coal Mining

To explore and analyze the active states of concealed crack structures and cracks in the deep floor, the KJ1073 micro-seismic system for coal mines, developed by the Hebei Coal Research Institute, was used to dynamically monitor the 2129 longwall face. The measurements provide data on the effectiveness of the water inrush control technology.

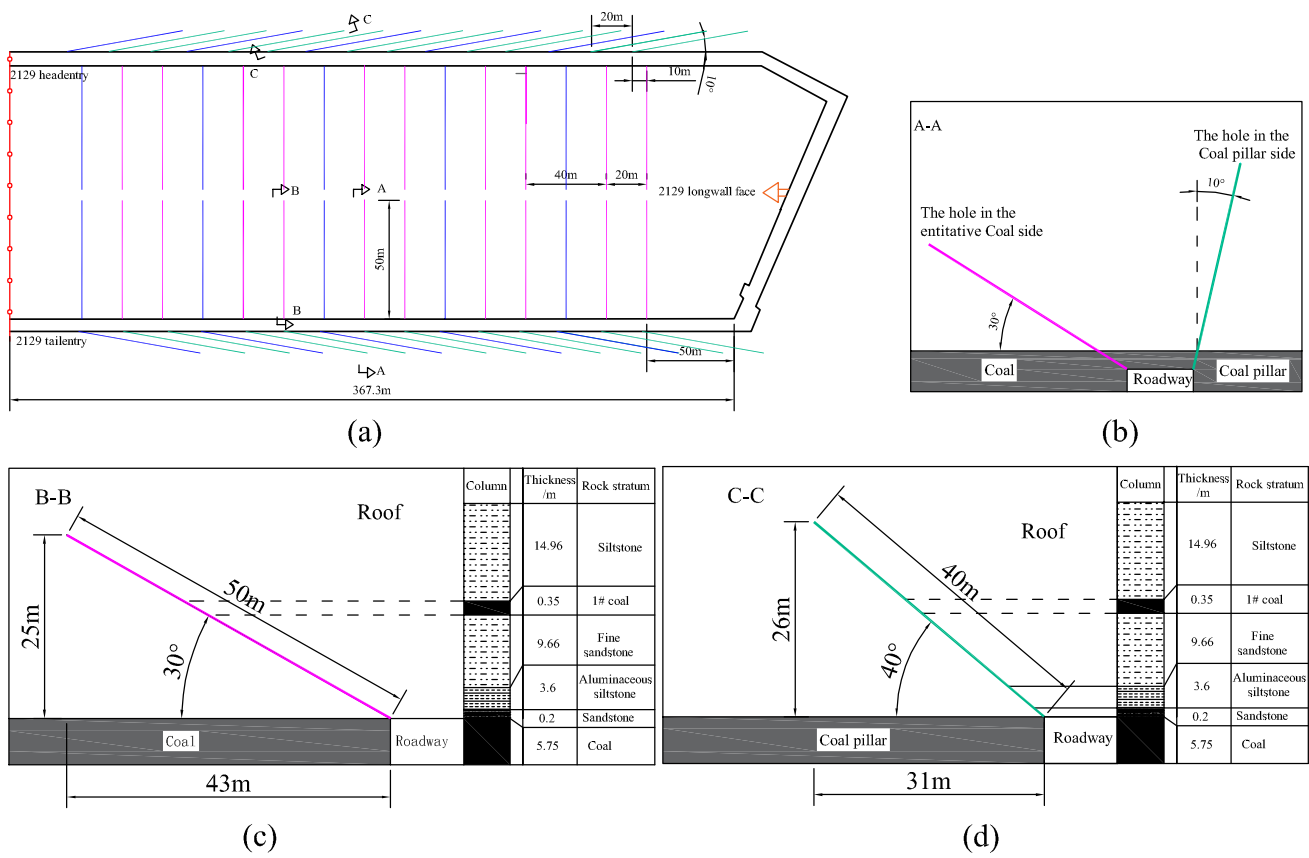


Fig. 8 Arrangement of boreholes presplitting roof for pressure relief at the 2129 longwall face: **a** Layout plan of boreholes. **b** A–A section. **c** B–B section. **d** C–C section

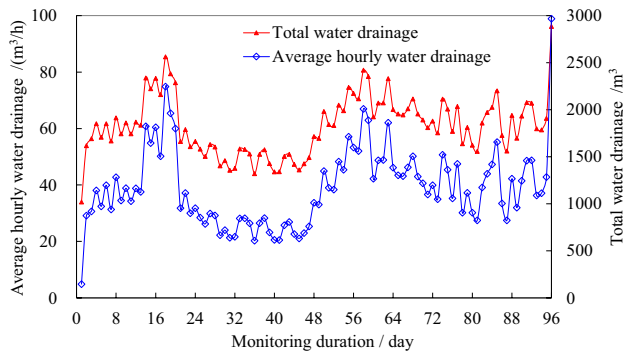


Fig. 9 Water drainage in the 2129 draining roadway

Dynamic Monitoring and Early Warning for Water Inrush

Spatial distribution maps of continuous microseismic events in the deep floor area from 09:00 on March 13 to 09:00 on March 16, 2019, are shown in Figs. 10 and 11. Figure 10 shows that microseismic events below the Yeqing limestone occurred in front of the longwall face from March 13 to March 16; the dense area of microseismic events remained

in the same position. Combined with Fig. 11, as the longwall face advanced, microseismic events in the deep floor area increased, and concealed crack structures began to connect from the shallow floor toward the deep Ordovician limestone. On March 13, microseismic events were mostly at shallower depths than the Yeqing limestone near the coal rib and were mostly deeper than the Yeqing limestone in front of the longwall face, about 50 m from the coal rib. From March 14 to March 15, the microseismic events moved toward the 2124 goaf. There was a constant increase in the magnitude of these events from the shallow floor to the Ordovician limestone. Hence, vertical cracks developed in the deep floor, and the water in the Ordovician limestone aquifer was moving.

The number of microseismic events in the floor area in front of the longwall face is plotted in Fig. 12. The microseismic events gradually increased in the section from the Yeqing limestone to the Fuqing limestone. They first increased and then decreased in each section deeper than the Fuqing limestone. In particular, there were more microseismic events in the Ordovician limestone than in the section from the Daqing limestone to the Ordovician limestone. These events reached a maximum on March

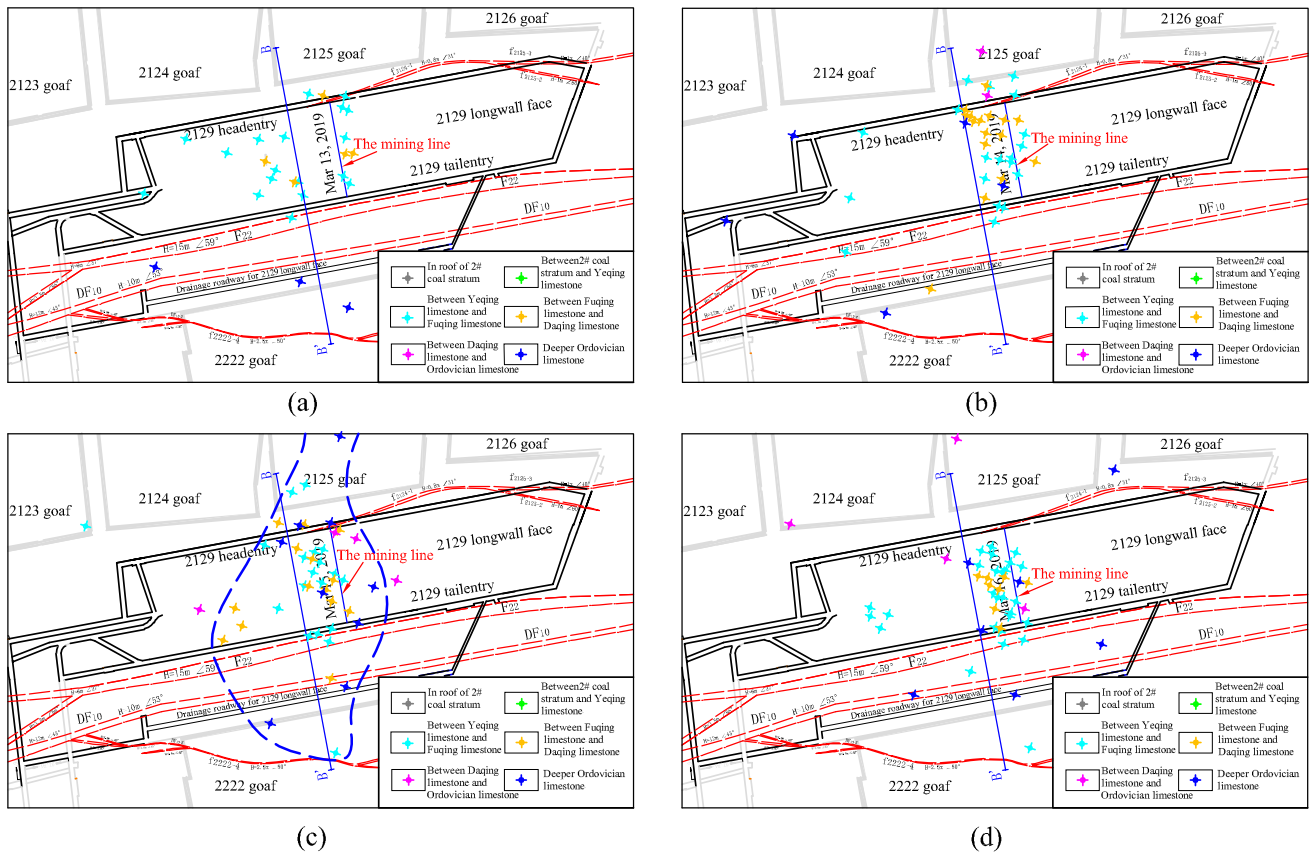


Fig. 10 Continuous evolution of microseismic events at floor area in front of longwall face—plan view: **a** March 13th, **b** March 14th, **c** March 15th, **d** March 16th

15, with the number of microseismic events in the Ordovician limestone rapidly increasing from five on March 14 to 15 on March 15; the number of microseismic events in the section from the Daqing limestone to the Ordovician limestone exhibited only a slight increase. After March 16, the microseismic events decreased below the Fuqing limestone.

When the longwall face crossed above concealed crack structures in the deep floor from April 2–5, the changes in the microseismic events were similar (see Figs. 10 and 11), and no water inrush disasters occurred through the floor. When the longwall face entered the central position from April 3–4, the number of microseismic events in each section of the floor area increased sharply. This basically signifies an interconnection from the shallow floor to the Ordovician limestone, making the risk of water inrush very high. Once the longwall face had crossed the region of concealed crack structures in the deep floor, fracture channels formed in the deep floor area below the goaf and the microseismic events basically disappeared below the Fuqing limestone on April 5. The change in the number of microseismic events in the floor area as the longwall face crossed the concealed crack structures is shown in Fig. 13.

The number of microseismic events first increased and then decreased in each section of the floor as the longwall face crossed the concealed crack structures. In particular, the number of microseismic events in the Ordovician limestone increased sharply from four on April 2 to 40 on April 4, much higher than in any section from the Yeqing limestone to the Ordovician limestone. The number of microseismic events in each section reached a maximum on April 4. The fewest events (only 14) occurred in the section from the Daqing limestone to the Ordovician limestone, although this was still 4.7 times greater than before the longwall face crossed the concealed crack structures on April 2. After the stresses of rock masses below the goaf unloaded and stabilized, the number of microseismic events in each section decreased rapidly from April 5 on.

Dynamic Monitoring for the Active State of Mining-induced Faults

Before mining, aquiclude faults can be discovered by geophysical exploration and drilling exploration. They easily fracture and actively form water-conducting channels when disturbed by mining, and their active state and fracture depth

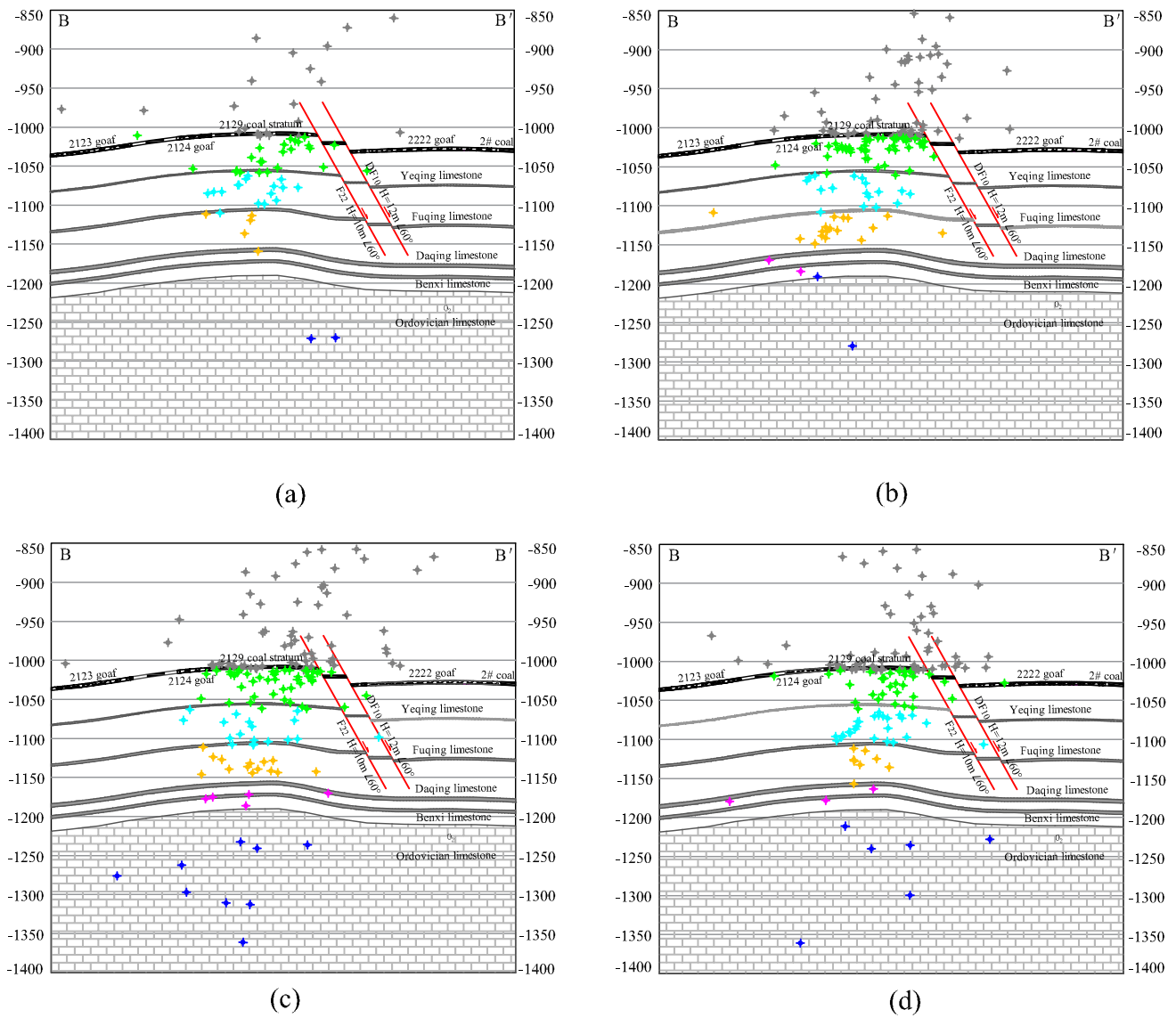
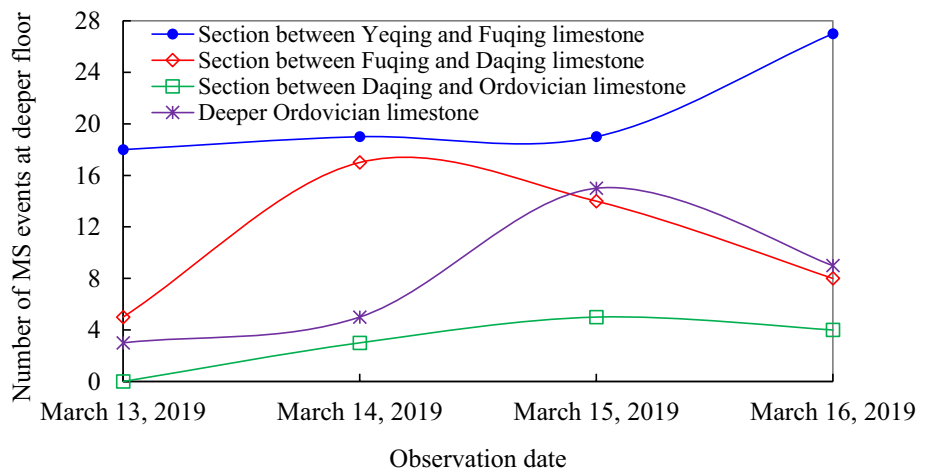


Fig. 11 Continuous evolution of microseismic events at floor area in front of longwall face—section view: **a** March 13th, **b** March 14th, **c** March 15th, **d** March 16th

Fig. 12 Number of microseismic events at floor area in front of longwall face



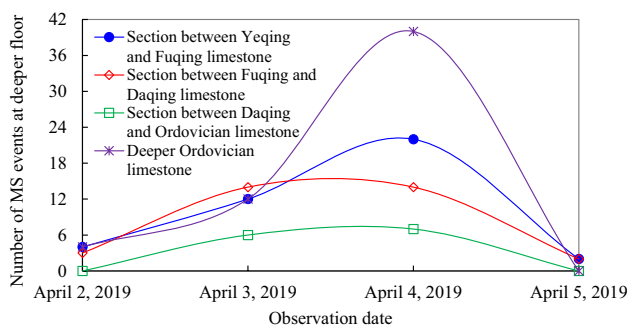


Fig. 13 Number of microseismic events at floor area with longwall face crossing concealed crack structures

is the key to connecting cracks to the Ordovician limestone deep below. The 2129 longwall face was close to the F_{22} and DF_{10} faults. The distribution of microseismic events near the fault region in 2129 longwall face is shown in Fig. 14.

Analysis of Figs. 10, 11, 12 indicates that most microseismic events occurred at the footwall of fault F_{22} from March 13–16. They were sporadically distributed in the hanging wall of fault F_{22} and both sides of fault DF_{10} , and were more likely to be located below the Yeqing limestone. On March 17, the number of microseismic events increased rapidly on both sides of faults F_{22} and DF_{10} , mainly below the Fuqing limestone, and they connected from below the 2129 longwall face to below the 2222 goaf. Moreover, the number of microseismic events in the section from the Yeqing limestone to the Fuqing limestone slowly increased from March 13–16, and then suddenly increased from 35 on March 16 to 83 on March 17; a notable increase was also observed in the section from the #2 coal seam to the Yeqing limestone. Hence, faults F_{22} and DF_{10} were fractured and active only below the Fuqing limestone, and there were few microseismic events

below the Fuqing limestone near either fault. There were no microseismic events at the bottom of the faults, and the microseismic events above and below the faults did not connect with the Ordovician limestone aquifer. Thus, dynamic microseismic monitoring shows that faults F_{22} and DF_{22} were not fully responsible for forming the water-conducting channels.

Danger Analysis of Water Inrush Through a Thick Aquifer Floor

Combining the information in Figs. 10, 11, 12, 13, 14, most microseismic events were distributed below the Fuqing limestone near both sides of fault F_{22} from March to April, and basically connected with the floor below the 2222 goaf. There were few microseismic events below the Fuqing limestone on either side of the faults. Hence, the number of microseismic events gradually decreased along the upper side of the fault toward the bottom of it. The critical depth near the fault under mining disturbances was near the Fuqing limestone. The microseismic events did not connect the top and bottom of the fault, and so the fault was not fully active and interconnected. Therefore, no water-conducting channels were formed.

The drop heights of F_{22} and DF_{10} are 10 and 12 m, respectively. The 2129 longwall face is located at the footwall of fault F_{22} , and the floor of the 2129 longwall face is about 22 m higher than below the 2222 goaf because of the footwall upward effect of the F_{22} and DF_{10} faults. Thus, cracks below the Fuqing limestone easily connected with the floor of the 2222 goaf. The dense microseismic events allowed fracture cracks to connect in the section from the shallow floor to the Ordovician limestone aquifer under the dynamic drainage and water pressure relief of the 2129 drainage

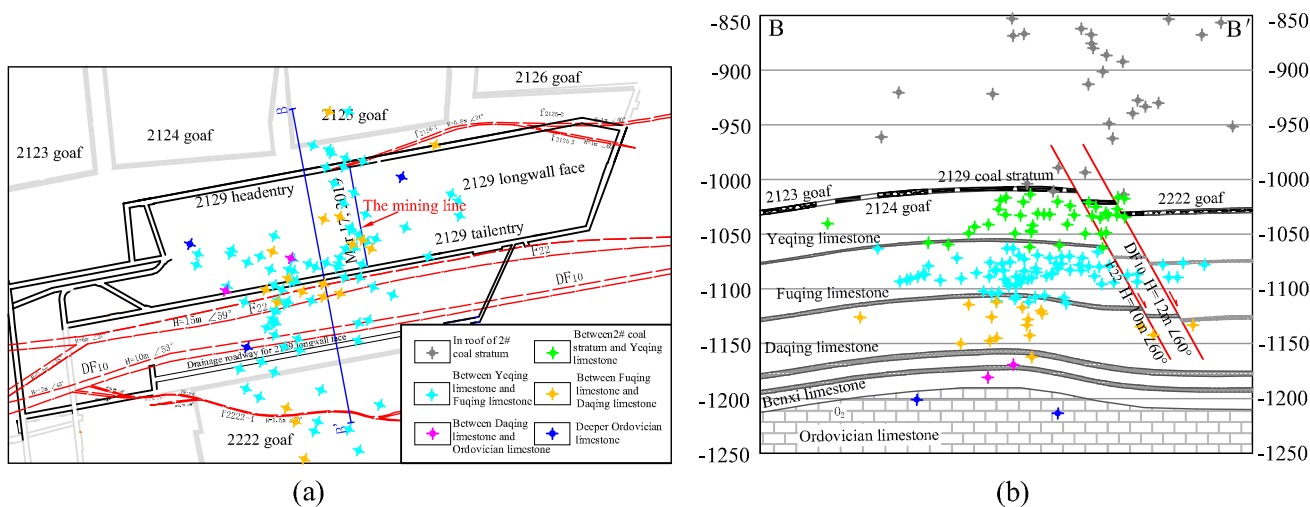


Fig. 14 Distribution of microseismic events near fault region in 2129 longwall face: **a** Plan view. **b** Section view

roadway. Even though water inrush occurred through the floor in the 2129 longwall face, this water flowed and discharged into the floor of the 2222 goaf, artificially lowering the danger of an inrush through the 2129 longwall face floor. This effectively relieved the water pressure and avoided a water inrush nearby.

Because of the grouting and reforming of the local floor, the grouted strata in the 2129 longwall face changed compared with the peripheral floor in the 2125, 2126, and 2222 longwall faces. The grouting boreholes were arranged to extend 220 m toward the south and 90 m toward the north of the 2129 longwall face, and they were all near the open-off cut and extended 93 m outside of the stopping line. The horizontal distance between boreholes was adjusted to 60 m, and the strata of grouting reinforcement were changed to be less than 50 m below the top surface of the Ordovician limestone, to enhance the grouting and reinforcement effects. Before the 2129 longwall face was mined, roof presplitting was performed to decrease the weighting interval; this relieved the pressure as the longwall face advanced. Moreover, the mining width of the 2129 longwall face was only 92.8 m, compared with 140–170 m for the other longwall faces at the –980 m level. This also reduced the underground pressure and lowered the stress disturbance intensity in the floor area.

The use of all of these control technologies in the 2129 longwall face prevented any water inrush disasters from occurring in the area. This approach could allow deep coal seams to be safely mined above high-pressure confined water.

Conclusions

The typical water inrush modes of thick aquifuge floor and stress disturbance modes acting on the floor area were obtained at the –980 m level in the deep Xing-dong coal mine in the north China coalfields based on the engineering background and field monitoring above confined water. Various control technologies for water inrush in the floor area in deep coal mining were tested. The results of microseismic monitoring and mining practices show that these control technologies can prevent water inrush through the floor. The main conclusions are as follows:

- (1) The water inrush modes were classified as either mining-induced cracks indirectly connected with the Ordovician limestone aquifer or through-going faults directly connected with the Ordovician limestone aquifer. The maximum water yield of the former takes a long time to reach a low value, while the latter reached a higher maximum in a short time.
- (2) The stress disturbance modes acting on the floor area in deep coal mines were divided into the dynamic load mode of the main roof instability from the far field of the longwall face and the static load mode of abutment pressure from the near field two types. The water yield of the former presented an obvious abrupt increase corresponding with the support loads and advance speed changes. And there is no obvious underground pressure in the longwall face for the latter.
- (3) The water inrush control technologies mainly include grouting and reinforcement with horizontal branch boreholes, decreasing the mining width, presplitting the roof to relieve the pressure, and dynamic drainage of confined water in the floor area.
- (4) As the longwall face advanced, microseismic events in the deep floor area increased, and cracks gradually connected the shallow floor with the deep Ordovician limestone. However, water inrush disasters did not occur through the thick aquifuge floor after using the inrush control technologies, allowing deep coal seams to be safely mined above high-pressure confined water.

Acknowledgements This work was supported by the National Natural Science Foundation of China (51904303), the Science and Technology Innovation Venture Capital Special Project of China Coal Research Institute (2021-KXYJ-004), and the Science and Technology Innovation Venture Capital Special Project of China Coal Technology & Engineering Group (2020-2-ZD001).

References

- Chen B, Zhang S, Li Y, Li Z, Zhou H (2020) Physical simulation study of crack propagation and instability information discrimination of rock-like materials with faults. *Arab J Geosci* 13:966
- Hu W, Zhao C (2021) Evolution of water hazard control technology in China's coal mines. *Mine Water Environ* 40:334–344
- Huang Z, Jiang Z, Tang X, Wu X, Guo D, Yue Z (2016) In situ measurement of hydraulic properties of the fractured zone of coal mines. *Rock Mech Rock Eng* 49:603–609
- Li H, Bai H (2020) Simulation research on the mechanism of water inrush from fractured floor under the dynamic load induced by roof caving: taking the Xinji second coal mine as an example. *Arab J Geosci* 12:466
- Li P, Li A, Wang X (2012) The comprehensive water control technology in the coal floor limestone high confined aquifer. *Adv Mater Res* 518–523:4283–4287
- Li Z, Feng G, Zhai C (2016) Study on “triangle” water-inrush mode of strong water-guide collapse column. *J Central South Univ* 23:2402–2409
- Li A, Ma Q, Lian Y, Ma L, Mu Q, Chen J (2020) Numerical simulation and experimental study on floor failure mechanism of typical working face in thick coal seam in Chenghe mining area of Weibei, China. *Environ Earth Sci* 79:118
- Liang Z, Song W, Liu W (2020) Theoretical models for simulating the failure range and stability of inclined floor strata induced by mining and hydraulic pressure. *Int J Rock Mech Min Sci* 132:104382
- Liu Y, Xia Y, Lu H, Xiong Z (2019) Risk control technology for water inrush during the construction of deep, long tunnels. *Math Prob Eng*. <https://doi.org/10.1155/2019/3070576>

- Lu H, Liang X, Shan N, Zhang Y (2018) Study on the stability of the coal seam floor above a confined aquifer using the structural system reliability method. *Geofluids*. <https://doi.org/10.1155/2018/9580271>
- Mu W, Wu X, Deng R, Hao Q, Qian C (2020) Mechanism of water inrush through fault zones using a coupled fluid–solid numerical model: a case study in the Beiyangzhuang coal mine, northern China. *Mine Water Environ* 39:380–396
- Sun J, Wang L, Hu Y (2019) Mechanical criteria and sensitivity analysis of water inrush through a mining fault above confined aquifers. *Arab J Geosci* 12:4
- Wu J, Jiang Z, Zhai X (2011) Research on controlling of rock mass structure on water inrush from coal seam floor in Huaibei mining area. 1st International Symp on Mine Safety Science and Engineering. *Proc Eng* 26:343–350
- Xiao L, Wu Q, Niu C, Dai G, Wang S, Ren D, Luo S (2020) Application of a new evaluation method for floor water inrush risk from the Ordovician fissure confined aquifer in Xiayukou coal mine, Shanxi, China. *Carbonates Evaporite* 35:97
- Xu Y, Yang Y (2013) Applicability analysis on statistical formula for failure depth of coal seam floor in deep mine. *Coal Sci Technol* 41(9):129–132 (**[in Chinese]**)
- Xu Y, Zhang E, Luo Y, Zhao L, Yi K (2020) Mechanism of water inrush and controlling techniques for fault-traversing roadways with floor heave above highly confined aquifers. *Mine Water Environ* 39:320–330
- Yin S, Zhang J, Liu D (2015) A study of mine water inrushes by measurements of in situ stress and rock failures. *Nat Hazards* 79:1961–1979
- Yin L, Ma K, Chen J, Xue Y, Wang Z, Cui B (2019) Mechanical model on water inrush assessment related to deep mining above multiple aquifers. *Mine Water Environ* 38:827–836
- Yu H, Zhu S, Xie H, Hou J (2020) Numerical simulation of water inrush in fault zone considering seepage paths. *Nat Hazards* 104:1763–1779
- Zhai J, Liu D, Li G, Wang F (2019) Floor failure evolution mechanism for a fully mechanized longwall mining face above a confined aquifer. *Adv Civ Eng*. <https://doi.org/10.1155/2019/8036928>
- Zhang J (2005) Investigations of water inrushes from aquifers under coal seams. *Int J Rock Mech Min Sci* 42:350–360
- Zhao J, Chen J, Zhang X, Jiang N, Zhang Y (2020) Distribution characteristics of floor pore water pressure based on similarity simulation experiments. *Bull Eng Geol Environ* 79:4805–4816
- Zou G, Hou S, Zhang K, Yin C (2010) Integrated water control technology for limestone water-inrush from coal floor fissures. In: *Proc 2nd international conf on mine hazards prevention and control*, vol 12. Atlantis Press, pp 379–388

Springer Nature or its licensor holds exclusive rights to this article under a publishing agreement with the author(s) or other rightsholder(s); author self-archiving of the accepted manuscript version of this article is solely governed by the terms of such publishing agreement and applicable law.